Geoderma 424 (2022) 115989

Contents lists available at ScienceDirect

Geoderma

journal homepage: www.elsevier.com/locate/geoderma

Soil meets stream: Vertical distribution of soil phosphorus in streambanks

Shengnan Zhou [a,b], Nan Li [a], Andrew J. Margenot [a,b,*]

[a] Department of Crop Sciences, University of Illinois Urbana-Champaign, Urbana, IL 61801, USA
[b] Agroecosystem Sustainability Center, Institute for Sustainability, Energy, and Environment, University of Illinois Urbana-Champaign, Urbana, IL 61801, USA

ARTICLE INFO

Handling Editor: Matthew Tighe

Keywords:
Streambanks
Soil phosphorus stratification
Pedogenic weathering
Fluvial erosion and deposition
Riparian land cover

ABSTRACT

Characterizing the vertical distribution of total phosphorus (P) and P forms in streambanks can improve estimates of P loads to streams via bank erosion. Using a systematic literature review, this meta-analysis evaluated the vertical distribution of total P (P_{tot}), Bray-1 test P (P_{Bray1}), oxalate-extractable P (P_{ox}), degree of P saturation (DPS_{ox}), and soil P storage capacity (SPSC) at 161 streambank locations encompassing diverse soil orders and riparian land covers. Across studies, maximum soil sampling depth (125 cm) was on average half that of streambank height (250 cm on average), and water quality-related P fractions such as water-extractable P (P_w) were not generally reported. Slightly weathered Entisols and Inceptisols collectively accounted for 84% of observations, likely reflecting alluvial deposition environments along stream corridors, and exhibited decreasing P_{tot} (820 to 400 mg kg^{-1}) with increasing depth to 200 cm. Irregular changes in P_{tot} at depth > 200 cm of Entisols and Inceptisols suggested burial of organic-rich A horizons by alluvial deposition. Changes in riparian land cover mainly affect P_{tot} in the upper 60 cm, with depth-weighted mean P_{tot} increasing as grassland (217 mg kg^{-1}) < forest (628 mg kg^{-1}) ≈ wetland (624 mg kg^{-1}) < developed (684 mg kg^{-1}) < agriculture (739 mg kg^{-1}), consistent with expected anthropogenic P enrichment of surface soils and posing increased P loading risk. Effect size analysis showed that riparian land cover had a large influence on P_{tot} within the top 30 cm depth whereas soil order and bedrock type had large influences on subsurface P_{tot}, suggesting depth-divergent drivers of P in streambank soils. Additionally, P_{tot} and P_{ox} were positively correlated with silt, clay, carbon, cation exchange capacity (CEC), oxalate-extractable iron (Fe_{ox}) and aluminum (Al_{ox}), and total Fe (Fe_{tot}) contents. This work helps advance understanding of the vertical variation of streambank soil P across diverse soil types, land covers, and soil properties, and their implications for P loading from bank erosion. We also identify gaps in sampling approaches (insufficient depth) and analysis (P_w) that may be hindering comprehensive assessment of bank erosion P loading and risk to water quality. Finally, we illustrate how fluvial erosion and deposition may generate complex vertical P distributions in streambanks, with implications for estimating erosional P loading that can benefit from a pedologically explicit approach.

1. Introduction

Streambanks are increasingly recognized as a large nonpoint source of phosphorus (P) to streams and rivers via bank erosion (Granger et al., 2021; Schilling et al., 2021), contributing 6 to 67% (Ishee et al., 2015; Peacher et al., 2018) and as high as 93% (Kronvang et al., 1997) of total riverine P and 21–42% of watershed diffuse P export (Kronvang et al., 2012). Mobilization and transport of P from streambanks can contribute to the eutrophication of receiving waters (Laubel et al., 2003; Sharpley et al., 2013). The magnitude of P loss from eroding banks and its influence on downstream water quality depends on P concentration in streambank material, not only total P but also readily desorbable (i.e., oxalate-extractable) P forms (Odhiambo et al., 2016; Perillo et al., 2021; Purvis et al., 2016; Young et al., 2012), which are often estimated by retrofitting agronomic soil P extractions (e.g., Bray-1) (Bray and Kurtz, 1945; Ishee et al., 2015; Young and Ross, 2016). Streambank total P can vary greatly with depth (e.g., 300–900 mg kg^{-1}) in an unpredictable manner (Ishee et al., 2015; Schilling et al., 2009), which can result in depth-variant P load and loss risk to streams. However, vertical P variability in streambanks has received little attention as many studies were limited to surface samples with typical depths less than 20 cm and/or depth-weighted mean P concentration (Beck et al., 2018; DeWolfe et al., 2004; Kessler et al., 2012). This may lead to underestimates of P loads from eroding banks (particularly bank undercuts) and its environmental

* Corresponding author at: 1102 S Goodwin Ave, Urbana, IL 61810, USA.
E-mail address: margenot@illinois.edu (A.J. Margenot).

https://doi.org/10.1016/j.geoderma.2022.115989
Received 11 January 2022; Received in revised form 11 April 2022; Accepted 6 June 2022
Available online 14 June 2022

risks to watershed water quality. In addition, given the proximity of bank faces to streams and the importance of geochemical processes on soil P supplies (Porder and Ramachandran, 2013), there is a need to understand deeper P concentrations of streambanks.

Streambanks are a key interface of terrestrial and aquatic systems (Pai and Saraswat, 2013), for which vertical P distribution can be complicated by coexisting weathering and stream dynamics, notably fluvial erosion and deposition. Generically, the form, amount, and variation of P in the soil profile are determined by underlying parent material (derived from rocks) and subsequent pedogenic soil-forming processes (e.g., illuviation) (Cross and Schlesinger, 1995). The Walker and Syers model (Walker and Syers, 1976) ascribes variation in total P – and its species – among soils to differences in weathering intensity and offers a basis for understanding vertical P distribution in streambanks to the extent that soils on streambanks are formed prior to the influence of flood events. For example, streambanks with more weathered soils (e.g., Alfisols) relative to less weathered soils (e.g., Inceptisols) would be expected to present lower concentrations of total P due to less readily soluble forms sorbed onto secondary minerals (Tiessen and Stewart, 1985). However, for streambanks with slightly weathered soils (e.g., Entisols and Inceptisols), total P concentration may not necessarily reflect weathering if these soils are formed by recent flood events and deposition of an alluvial mantle. In addition, alluvium on banks with Entisols or Inceptisols soils could originate from more weathered soils eroded from upstream, entailing lower total P content than anticipated by the Walker-Syers model (Walker and Syers, 1976). The newly formed alluvial soils on streambanks can also be removed by subsequent fluvial erosion (Boettinger, 2005; Terence, 1987). Therefore, streambank material characteristics (e.g., texture and bulk density) may exhibit a high degree of variability with depth, and banks in alluvial streams often have numerous stratigraphic layers differing in fineness to coarseness (Beck et al., 2018; Layzell and Mandel, 2014). Preferential enrichment of P in fine soil particles by virtue of phosphate-clay interactions drives a high degree of variability of streambank P content by depth (Moustakidis et al., 2019).

In addition to weathering interacting with fluvial erosion and deposition, streambank P concentrations are concurrently influenced by local riparian land uses and land covers (Perillo et al., 2019; Tufekcioglu, 2010; Zaimes et al., 2019). Agricultural land uses (e.g., cultivated crops and pastures) can elevate P concentration in the surface soil due to net inputs from fertilizer (Tran and N'dayegamiye, 1995) or manure (Abdala et al., 2015; MacDonald et al., 2011). Net P addition from past agricultural management can result in legacy P accumulation in the upper bank (Rowe et al., 2016; Sharpley et al., 2013), increasing P export potential to streams via bank retreat or mass failure (McDowell et al., 2001; Stackpoole et al., 2019). Additionally, vegetation (e.g., trees, shrubs, grasses) and wetlands in riparian buffers can trap dissolved reactive P in runoff and sediments (Hoffmann et al., 2009), leading to decreased total P with depth (Huang et al., 2015). However, forest, grassland, or wetland buffers generally still have appreciably lower surface P concentration than those under agricultural use for a given edaphoclimatic context (Chai et al., 2015; Houlahan and Findlay, 2004).

The goal of this study is to evaluate the vertical distribution of total P and P forms in streambanks using a systematic literature review and meta-analysis approach. We (i) evaluated the published studies of P vertical variation in streambanks to identify potential reporting or measurement gaps; (ii) examined in detail the streambank P variation with depth under different soil orders and riparian land covers; (iii) assessed the influence of other environmental factors (climate region, parent material, bedrock type) and soil properties on streambank P content; and (iv) evaluated limitations and implications of this work. To address these objectives, we conducted a systematic literature review and meta-analysis of published soil P profiles of streambanks supplemented with the US Department of Agriculture (USDA) National Cooperative Soil Survey (NCSS) dataset, encompassing differing soil types and riparian land covers in the context of diverse climate regions, parent material, and bedrock types. By integrating soil science with stream hydrology, this study offers insights into vertical P distribution of streambanks and provides typical ranges of P values found in various streambanks worldwide which could be useful in evaluating watershed sediment P loads studies.

2. Materials and methods

2.1. Data sources

To synthesize peer-reviewed articles on vertical P profiles on streambanks and relationships with bank erosion, we conducted a systemic literature search on the Web of Science in July 2021. The following search terms were used in the "Advanced Search/All Fields": ("streambank erosion" OR "bank erosion" OR "riverbank erosion") AND ("phosphorus*" OR "phosphate*" OR "P") AND ("soil*" OR "sediments*" OR "riparian" OR "buffer*" OR "floodplain*" OR "vertical distribution*" OR "stratigraphy*" OR "stratification*" OR "parent material" OR "lithology*" OR "pedogenesis*" OR "soil age*" OR "soil chronosequence*"). Note that the "*" symbol next to each search term retrieves variants of this term. To ensure thorough coverage of literature, a similar search was conducted in August 2021 using the Scopus database. The two searches resulted in 453 records (Web of Science, n = 324; Scopus, n = 120). After excluding duplicates, we evaluated a net total of 384 abstracts and identified 101 of these as having soil P observations on streambanks and with full-text availability. Of these 101 articles, we further restricted the soil P search to 18 articles that reported streambank P content for at least three depth ranges, from which 93 soil profiles were identified (Fig. S1).

To maximize the comprehensiveness of the final *meta*-dataset, the 93 soil profiles collected from the published articles were merged with another 68 soil profiles on first order-up streams across the US obtained from the USDA-NCSS database (Fig. S2). Of these 68 NCSS sampled sites, 26% were on the actual streambanks, 25% were within 1–9 m from the banks, and 25% were within 11–39 m from the banks (Fig. S2). Though the last 24% were beyond 46 m from the banks, the Web Soil Survey mapped units were centered on these sampled locations and extended to the nearest stream edges thus can represent the soil types on the banks. Site information and soil characterization data of these soil profiles were retrieved from the NCSS Lab Data Mart Point Database by executing sequential queries in Microsoft Access (O'Geen et al., 2017). The final dataset comprised 161 soil profiles with 945 soil samples (Fig. S1).

2.2. Data collection

For each entry in the *meta*-database, the following information was collected (if available): (i) spatial location (country, name of the area, coordinates); (ii) mean annual temperature and precipitation; (iii) channel and streambank characteristics, including channel name, channel length (km), drainage area (km^2), and streambank height (cm); (iv) soil type, parent material, and bedrock type; (vi) land cover type on the bank; (vi) soil data, including the top and bottom boundaries of soil sample depth (cm), horizons, total P (P_{tot}), bioavailable soil-test P, oxalate-extractable P, Iron, and aluminum (P_{ox}, Fe_{ox}, Al_{ox}), texture (sand, silt, and clay contents), pH, total (organic) carbon content (C_{tot}, %), cation-exchange capacity (CEC), and total Ca, Fe, and Al (Ca_{tot}, Fe_{tot}, Al_{tot}) content. Though bulk density is an important variable for determining streambank P stocks, it was excluded from the analysis due to insufficient reports (20% of the observations). This was also the case for water-extractable P (P_w).

The missing site coordinates were estimated by searching reported channel names and location names using Google Maps. Missing mean annual temperature and precipitation data were extracted from the WorldClim database using ArcGIS Pro (Fick and Hijmans, 2017). The temperature and precipitation combinations were assigned to one of the

18 world climate regions (Fig. 1) developed by Sayre et al. (2020). Missing channel length and drainage area were measured from reported watershed maps with WebPlotDigitizer (Drevon et al., 2017) or obtained from Wikipedia. Soil type was categorized by USDA soil order with the conversion from the FAO classification system as needed (Bockheim et al., 2014; Staff, 1999). Parent material (1974, 1:20000 mapping) from the USDA Natural Resource Conservation Service Soil Survey Geographic Database (NRCS SSURGO) (Staff et al., 2021) was used to assign each sampling point to one of the following categories: alluvium, glaciolacustrine, glaciofluvial, glacial till, outwash, loess, and residual. Bedrock type of the region surrounding the stream channels, used to evaluate parent material P content, was collected from the State Geologic Map Compliance (SGMC) Geodatabase (Horton, 2017) and further grouped into the following categories based on Suchet et al. (2003): acid volcanic, basalt, carbonate, sandstone, shale, and shield. Total P concentrations of these bedrocks (P_{rock}) were obtained from reported values by Porder and Ramachandran (2013) to assess parent material P influence on soil P concentrations. For the US studies, missing information on riparian land cover was collected from the US Geological Survey (USGS) National Land Cover Database (NLCD) (Wickham et al., 2021). The land cover type was classified as forest (evergreen forest, deciduous forest, mixed forest, and shrubs), grassland (native grass and herbaceous plants), wetland (woody wetlands and emergent herbaceous wetlands), agriculture (pasture and cultivated crops), or developed (open space, residential, and commercial).

All depth-wise soil data were extracted from reported tables and graphs using WebPlotDigitizer (Drevon et al., 2017). Values reported as P_2O_5 were converted to P (Lambers and Barrow, 2020). The Bray-1P (P_{Bray1}) test is recommended for circumneutral to highly acidic soils (Mallarino, 1995). Given that 91% of reported pH values were equal to or <7.4, the P_{Bray1} or P_{Bray1} equivalent converted from Modified Mogan's P (Ketterings et al., 2002) or Mehlich-3P (Culman et al., 2019) was used for the final analysis. Soil pH was expressed as pH measured in water, with the conversion of pH measured in a background solution of $CaCl_2$ applied as necessary (Ahern et al., 1995). Soil total carbon (C_{tot}) was interpreted as total soil organic carbon if the reported pH was < 7.2 (Stott, 2019). If only soil organic matter was reported, the value was divided by 1.72 to estimate soil organic carbon content (Pribyl, 2010). The degree of P saturation (DPS) is commonly used in evaluating the risk of P loss from soil to the environment (Odhiambo et al., 2016; Pradhan et al., 2021) and is useful for understanding short-term P release to water bodies following bank erosion. The degree of P saturation (DPS_{ox}, %) was calculated as the ratio of P_{ox} to (Fe_{ox} + Al_{ox}) (Nelson et al., 2005):

$$DPS_{ox}(\%) = \frac{P_{ox}}{0.5 \times (Fe_{ox} + Al_{ox})} \times 100 \quad (1)$$

where P_{ox}, Fe_{ox}, and Al_{ox} are oxalate-extractable phosphorus, iron, and aluminum (mg kg^{-1}).

However, DPS_{ox} does not indicate the capacity of soil to retain added P (Nair and Harris, 2004) and therefore the index of soil P storage capacity (SPSC) was used as a proxy of the amount of P streambank soil can retain via sorption. SPSC provides a meaningful indicator of P-related environmental risk by accounting for the amount of P that can be added to the soil before the soil retention capacity for orthophosphate is exceeded and thus presents a P loss risk (Nair and Harris, 2004). The SPSC (mg kg^{-1}) was calculated using the generalized equation by Nair (2014):

$$SPSC = (\text{Threshold PSR} - \text{Soil PSR}) \times (Fe_{ox} + Al_{ox}) \times 31 \text{ mg kg}^{-1} \quad (2)$$

where PSR is P saturation ratio; threshold PSR is assumed as a constant of 0.1 according to Nair (2014); soil PSR equals DPS_{ox}; Fe_{ox} and Al_{ox} are oxalate-extractable iron and aluminum (mg kg^{-1}); and 31 mg kg^{-1} is the correction factor, according to Nair (2014). The SPSC value indicates whether the streambank soil is a net P sink (positive) or net P source (negative).

2.3. Statistical analyses

The vertical profiles of streambank P variables (P_{tot}, P_{Bray1}, P_{ox}, P_{ox}/P_{tot} ratio, DPS_{ox}, and SPSC) were vised using the R *aqp* (algorithms for quantitative pedology) package (Beaudette et al., 2021). The *apq*

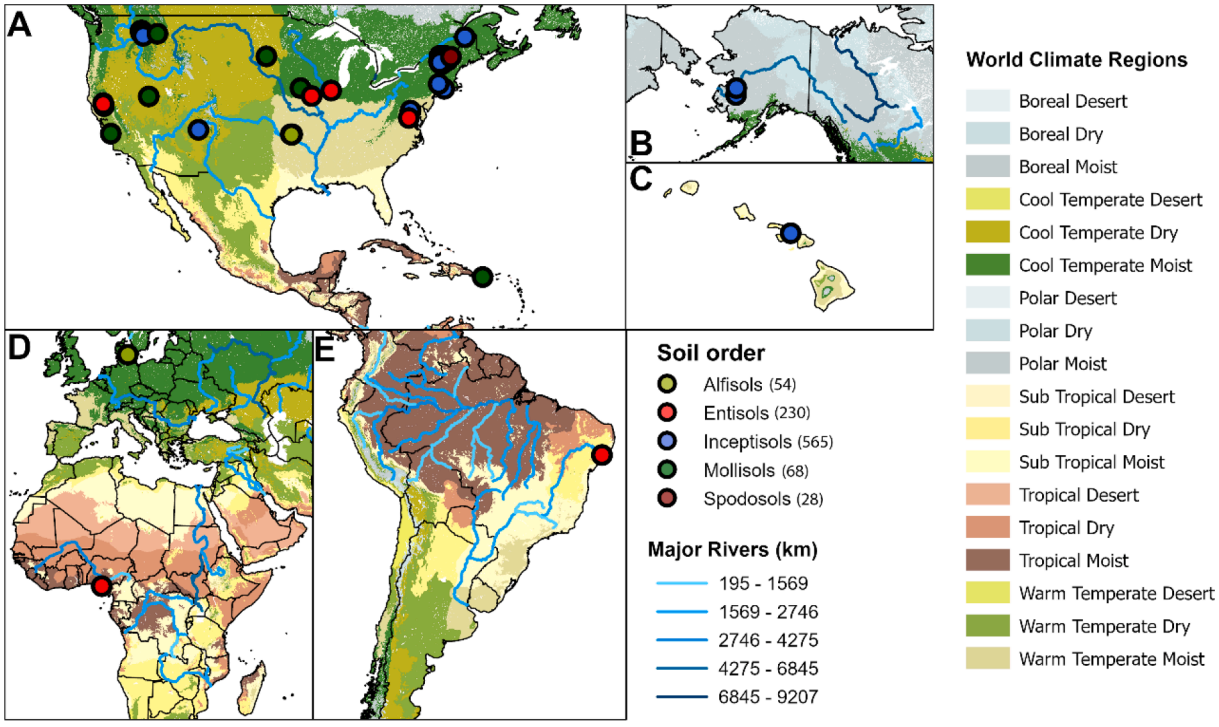

Fig. 1. Spatial distribution of streambank soil observations by USDA soil order within (A) contiguous US, (B) Alaska, US (C) Hawaii, US (D) Europe and South Africa, and (E) South America. Parentheses after the soil order name show the total number of soil samples in each class.

package embeds a slice-wise aggregation algorithm aligned the P property from each profile to a common depth basis by slicing the data into 1-unit spaced intervals ranging from the minimum to maximum profile depth (Beaudette et al., 2021). Summary statistics (e.g., mean, standard deviation, or quantiles) were computed along with slices across the collection of profiles.

Since the maximum sampling depth of the studies averaged approximately 120 cm, for comparability among different streambanks, the upper 120 cm subset at 15-cm depth intervals was used to test depth-wise differences in soil P variables using post-hoc multiple means comparisons. First, data were tested for assumptions of analysis of variance (ANOVA) using the Shapiro-Wilk test for normality of residuals at a significance level of 0.05 using the *shapiro.test()* function from the R *stats* package (R Core Team, 2021). Since P variables by soil order or land cover were not normally distributed, the non-parametric Kruskal-Wallis test was performed for mean differences using the *kruskal.test()* function (R Core Team, 2021), followed by the Dunn rank test with Bonferroni correction (adjusted p-values for multiple comparisons) using the *DunnTest()* function from the R *FSA* package (Ogle et al., 2021).

The standard effect size of environment factors (climate region, parent material, bedrock, soil order, and riparian land cover) to the results (P_{tot}, P_{Bray1}, P_{ox}, P_{ox}/P_{tot} ratio, DPS_{ox}, SPSC) was tested at 15-cm depth intervals to 120 cm depth. For this, we used the index of eta-squared based on the H-statistic (eta2[H]) using the R *kruskal_effsize()* function (Tomczak and Tomczak, 2014). The eta2[H] is an effect size measure used in the context of analysis of variance, as an analog of the parametric F-test in ANOVA, and is calculated as (Tomczak and Tomczak, 2014):

$$\text{eta2[H]} = \frac{H - k + 1}{n - k} \quad (3)$$

where H is the value obtained in the Kruskal-Wallis test; k is the number of groups; n is the total number of observations. A eta2[H] $>$ 0.14 is considered a large effect size, 0.06–0.14 a moderate effect size, and $<$ 0.06 a small effect size (Tomczak and Tomczak, 2014). We also evaluated the relationships among streambank P variables and soil properties using Spearman's rank correlation coefficient test with visualization using the R *corrplot* package (Wei and Simko, 2021).

3. Results

3.1. Summary statistics and aggregated data

The compiled dataset comprised 161 streambank soil profiles in 41 first- to tenth-order streams (Strahler, 1957) (Fig. S3) from the continental US (Fig. 1A) and US states or territories of Alaska (Fig. 1B), Hawaii (Fig. 1C) and Puerto Rico (Fig. 1A), as well as Denmark, Nigeria (Fig. 1D), and Brazil (Fig. 1E). Eighty-five percent of the soil profiles were in the US partially due to the contribution of the NCSS dataset and 86% of the profiles were in third- to sixth-order streams (Fig. S3). We did not find peer-reviewed studies or unpublished data of streambank P profiles for Asia and Australia. Nonetheless, these sites encompassed a variety of climate regions including tropical, subtropical, warm and cool temperate, and boreal (Fig. 1), with mean annual temperature ranging from −2.3 to 26.6 °C and mean annual precipitation of 272 to 1885 mm (Table 1).

When classified into low, intermediate, and high weathering based on the criteria reported by Yang and Post (2011), the 161 soil profiles were largely comprised of lowly weathered Entisols (24%) and Inceptisols (60%) and to a lesser extent intermediately weathered Mollisols (7%), Alfiosls (6%), and Spodosols (3%). The riparian land cover of the observations was dominated by agriculture (47%), forest (31%), and wetlands (15%). Thus, the soil order and land cover variation entailed diverse soil properties. Soil pH varied from strongly acidic (pH $<$ 5) with a minimum of 2.4 to moderately alkaline (pH $>$ 7) with a maximum of 8.7, and 84% of the soil pH observations were acidic ($<$7) with a mean of 6.1. Soil C_{tot} content varied by more than three orders of magnitude from 0.02% to 53.8%, with a mean of 1.4% (Table 1). The texture of these observations was dominantly coarse, with 55% of the soils having $>$ 50% sand content and categorized as the sandy textural class (Table 1). The parent material of these soils was dominated by alluvium (77%) followed by glaciolacustrine deposit material (10%) and glacial till (5%). The bedrock in the regions of the observations included 43% shields, 24% carbonates, 22% sandstone, 7% basalt, and 4% shale, with total rock P concentration ranging from 289 to 1047 mg kg^{-1} and mean of 593 mg kg^{-1} (Porder and Ramachandran, 2013).

Diversities of geophysical environment and soil properties entailed large variations in streambank P forms and contents (Table 1). The values of P_{tot}, followed by P_{ox}, showed the largest variation with a mean

Table 1
Summary statistics of mean annual temperature (MAT) and precipitation (MAP), study duration, streambank characteristics, soil properties, and soil P variables. P_{rock}, P_{tot}, P_{Bray1}, P_{ox}, P_w correspond to bedrock P, soil total P, Bray-1 test P, oxalate-extractable P, and water-soluble P, respectively.

Variable	[1] N	[2]n	Mean	SD	Median	Min	Max
MAT (°C)	161		7.8	4.0	6.7	−2.3	26.6
MAP (mm)	161		949.2	190.3	984.0	272.0	1885.0
Measured duration (yr)	92		2.7	1.9	2.0	0.1	10.0
Stream length (km)	153		176.7	600.5	27.8	3.1	4180.0
Drainage area (km^2)	137		4.3×10^4	2.2×10^5	181.3	16.0	2.1×10^6
Bank height (cm)	67		254.5	139.0	200.0	30.0	600.0
Maximam sample depth (cm)	161		125.5	49.2	120.0	24.0	360.0
Soil sample depth (cm)		945	73.4	54.2	60.0	2.5	360.0
Sand (%)		711	50.3	27.0	53.2	0.3	98.3
Silt (%)		711	38.0	20.2	36.3	1.0	86.4
Clay (%)		694	11.9	11.9	7.7	0.1	71.8
C_{tot} (%)		759	1.4	3.3	0.7	0.02	53.8
pH (water)		620	6.1	1.0	6.1	2.4	8.7
P_{rock} (mg kg^{-1})	161		593.2	116.1	600.0	289.0	1047.0
P_{tot} (mg kg^{-1})		821	660.0	249.3	666.0	1.0	1874.0
P_{Bray1} (mg kg^{-1})		718	11.0	18.3	4.3	0.1	180.7
P_{ox} (mg kg^{-1})		470	263.7	159.2	235.6	1.0	1077.9
P_{ox}/P_{tot} ratio		463	0.39	0.18	0.36	0.01	0.95
DPS_{ox} (%)		494	12.5	6.9	11.6	0.1	48.6
SPSC (mg kg^{-1})		422	1350.3	15,215	−837.0	−33659	1.1×10^5
P_w (mg kg^{-1})		124	1.9	2.6	0.2	0.1	9.0

[1] N: the number of observations at the profile level. N total = 161.
[2] n: the number of observations at the soil sample level. n total = 945.

of 660 mg kg^{-1} and a standard deviation of 249 mg kg^{-1}. The agronomic measurement of P_{Bray1} showed a smaller range in values (0.1–180.7 mg kg^{-1}) with a mean of 11.0 mg kg^{-1} and a standard deviation of 18.3 mg kg^{-1}. The P_{ox}/P_{tot} ratios varied largely from 0.01 to 0.95 with a mean of 0.39. DPS_{ox} varied from 0.1% to 48.6 % with a mean of 12.5%, and SPSC ranged from -3.7×10^4 to 1.1×10^5 mg kg^{-1} with a mean of 1350 mg kg^{-1}. The profile depth (the distance between the top and the bottom depths of a profile) of the studies ranged from 24 to 360 cm with a mean of 125 cm, while the streambank mean height was double that with a greater range of 30–600 cm (Table 1). Though 91% of the soil sampling depths were shallower than 150 cm, 87% of the reported streambank height exceeded 150 cm (Fig. 2).

3.2. Vertical P distribution in streambanks by soil orders

Variations in streambank P variables with depth under different soil orders were broadly supportive of the expected differences in P stratification under different weathering states inferred by soil classifications (Fig. 3 and Fig. S4). The P_{tot} concentration in Entisols decreased (from 640 to 400 mg kg^{-1}) with increasing soil depth in the upper 150 cm of the profile and then increased up to 800 mg kg^{-1} at a depth of 240 cm. For Inceptisols, P_{tot} continuously declined from a surface concentration of 820 mg kg^{-1} to 700 mg kg^{-1} at 175 cm, followed by a two-fold (400 mg kg^{-1}) reduction at the bottom depth of 240 cm. Inceptisols also exhibited significantly higher P_{tot} in the upper 120 cm compared to other soil orders (Fig. S5A). In Mollisols, P_{tot} concentration fluctuated throughout the profile with less variation (400–600 mg kg^{-1}) in the upper 120 cm than in deeper depth (300–900 mg kg^{-1}). Alfisols and Spodosols had a similar P_{to} distribution pattern with depth, which were relatively constant around 400–500 mg kg^{-1} in the upper 50 cm and then increased to 610 mg kg^{-1} at 75–150 cm depth.

The concentration of P_{Bray1} was similarly low (<10 mg kg^{-1}) across all soil orders (Fig. 3). However, surface (15 cm) P_{Bray1} in Mollisols was about six-fold higher (30 mg kg^{-1}, Fig. S1B) than in other soil orders (<5 mg kg^{-1}, Fig. S5B). Notably, P_{Bray1} at 150–240 cm of Entisols and Inceptisols increased by six- to ten-fold compared to the depth above 150 cm. The vertical distribution of P_{ox} did not reflect weathering intensity of soil orders, being lowest in Spodosols, intermediate in Entisols and Inceptisols, and highest in Alfisols. The P_{ox} concentration in Entisols and Inceptisols profiles generally varied in the same manner as P_{tot}. Though limited in the number of observations, P_{ox} in Mollisols decreased from 390 to 120 mg kg^{-1} with increasing depth from 0 to 80 cm, but was relatively constant in Alfisols except for local maxima of 480 mg kg^{-1} at 20 cm and local minima of 300 mg kg^{-1} at 90–110 cm. The depth distribution of P_{ox}/P_{tot} ratios varied greatly among soil orders and strongly reflected differences in P_{ox}, ranging from 0.05 to 0.25 in Spodosols to 0.40–0.60 in Alfisols.

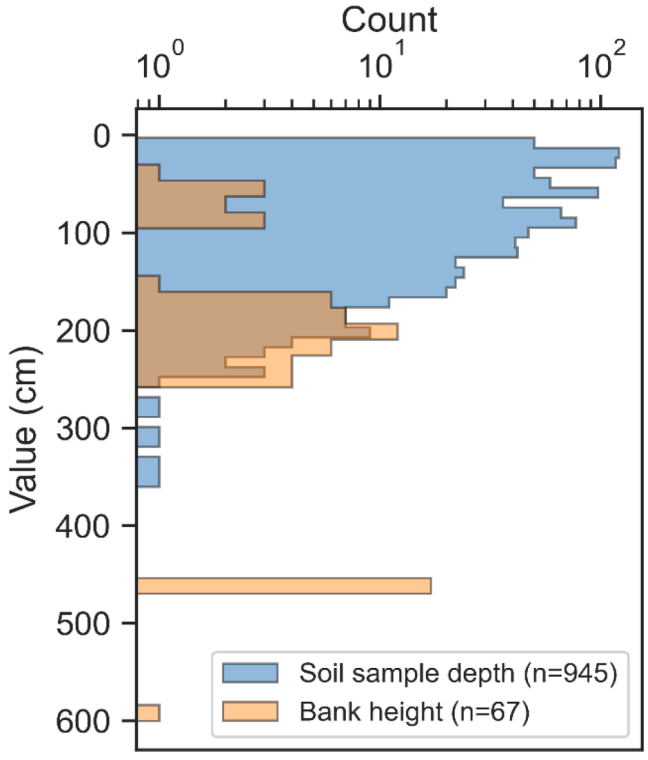

Fig. 2. Distribution of soil sample depth and bank height collected from the systematic literature review and USDA NCSS database.

DPS_{ox} in the top 20 cm ranged from 5% in Spodosols to 22% in Mollisols. As soil depth increased, DPS_{ox} was found to decrease in Mollisols but increase in Alfisols, resulting in the highest DPS_{ox} (15–22%) in the subsurface (50–150 cm) of Alfisols. Though DPS_{ox} in Entisols and Inceptisols were relatively constant (10%) between 50 and 150 cm depth, it increased appreciably (25%) at 200 cm for both soil types. The SPSC index indicates net P source when SPSC < 0 and net P sink when SPSC > 0. In the top 20 cm depth, negative SPSC values ranged from −2000 mg kg^{-1} in Inceptisols to −15000 mg kg^{-1} in Mollisols, suggesting weak to very strong net potential as P sources. Positive SPSC values, and thus potential P sinks, ranged from 1000 mg kg^{-1} in Entisols to 5000 mg kg^{-1} in Spodosols to 10000 mg kg^{-1} in Alfisols. Alfisols transitioned from sink to source of P at a depth of approximately 50 cm, whereas Spodosols appeared to be P sink throughout all depths (to 120 cm).

3.3. Vertical P distribution in streambanks by riparian land covers

The vertical patterns of streambank P differed less by riparian land covers than by soil orders (Fig. 4). Specifically, P_{tot} concentration differed more significantly among land covers in the upper 60 cm of all profiles than below 60 cm (Fig. S6A). At 0–30 cm depth, there was the highest P_{tot} concentration under agriculture (800–900 mg kg^{-1}), followed by wetland (700–800 mg kg^{-1}), forest, and developed lands (700 mg kg^{-1}), and was lowest under grassland (320–520 mg kg^{-1}). The P_{tot} concentration under forest decreased slightly from 660 to 600 mg kg^{-1} as soil depth increased from 0 to 60 cm, followed by a dramatic reduction to 400 mg kg^{-1} before increasing back to 800 mg kg^{-1} at the bottom depth of 240 cm. In contrast, P_{tot} under grassland increased from 400 to 600 mg kg^{-1} with soil depth increasing from 0 to 60 cm and then declined rapidly throughout the rest of the depth. There was a similar declining trend of P_{tot} with increasing soil depth under wetland and agricultural land, except that P_{tot} under agricultural land increased by 20% at 160 cm before abruptly decreasing by 50% at 160–190 cm. Though observations were limited, P_{tot} in developed lands varied from 520 mg kg^{-1} at 25–45 cm to 800 mg kg^{-1} at 140–150 cm. In contrast, P_{Bray1} in the upper 200 cm was generally low (<20 mg kg^{-1}) and varied little across land covers. However, P_{Bray1} concentration under forest and agriculture increased by three to six-fold at 160–240 cm relative to the upper depth.

The amount of P_{ox} generally increased with increasing human intervention to the soil system proxied by riparian land covers, particularly in the upper 60 cm (Fig. 4 and Fig. S6C): forest < wetland < agriculture < developed. P_{ox} concentration in the upper 200 cm of wetland, agriculture, and developed soils exhibited decreasing trends as soil depth increased. However, some irregular patterns were observed within the soil profiles associated with developed land uses with local maxima of 375 mg kg^{-1} at 45–55 cm and local minima of 100 mg kg^{-1} at 115–130 cm. In contrast, P_{ox} of forest soils remained relatively constant (200 mg kg^{-1}) to the 200 cm depth. The highest P_{ox} concentrations (≈475 mg kg^{-1}) existed in the forest and agriculture soils at 200 cm depth. Overall, streambanks with wetland and developed lands had higher P_{ox}/P_{tot} ratios than forest and agriculture lands, especially in the upper 120 cm (Fig. S6D). The vertical distribution patterns of P_{ox}/P_{tot}

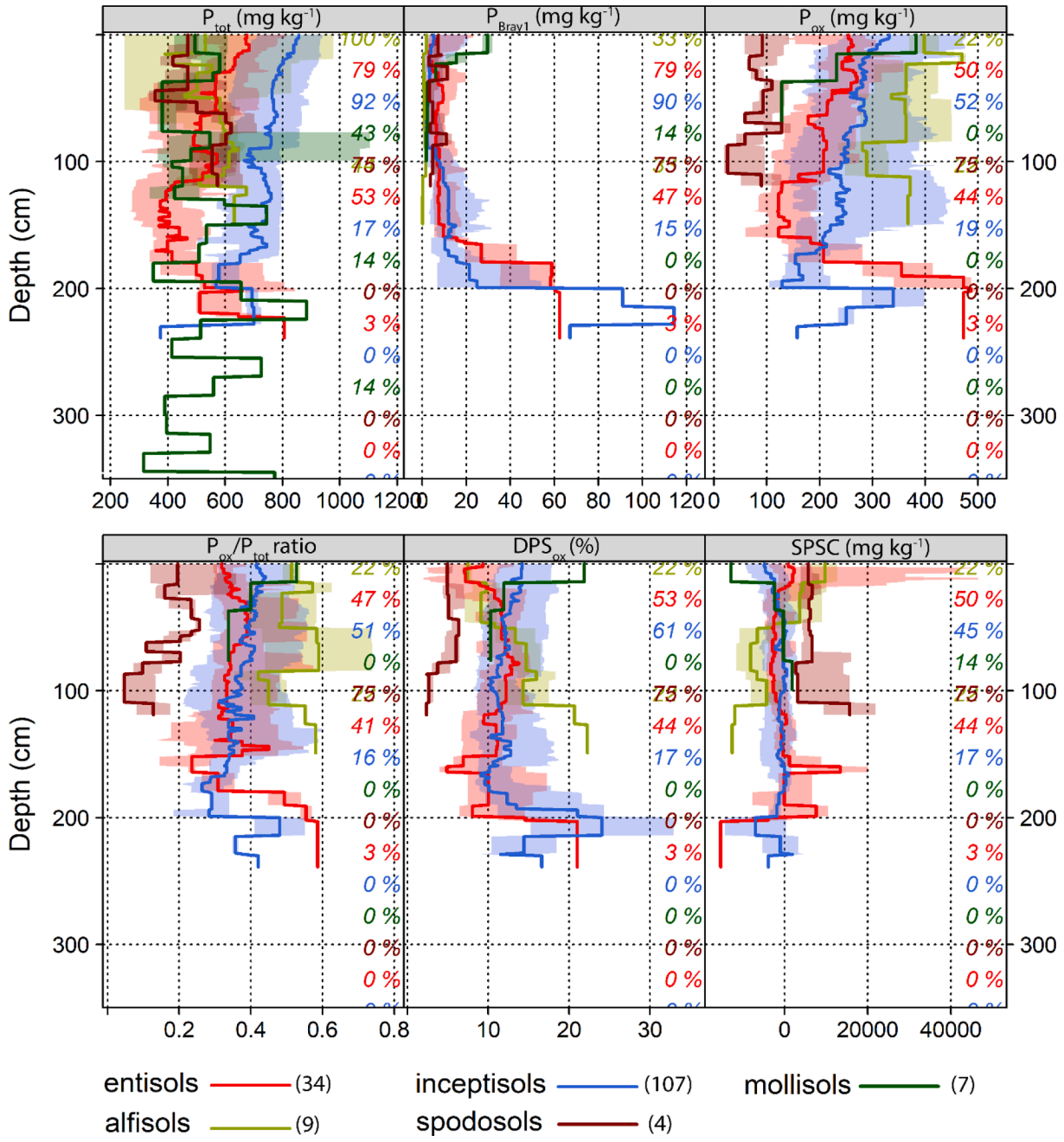

Fig. 3. Vertical profiles of P_{tot}, P_{Bray1}, P_{ox}, P_{ox}/P_{tot} ratios, DPS_{ox}, and SPSC in streambanks by soil orders. Solid lines are median values bounded by the interval defined by the 25th and 75th percentiles. Parentheses after the soil order name show the total number of soil profiles for each order. Values along the right-hand side y-axis describe the proportion of total profile observations with values reported at a given depth. An increasing weathering arranged soil orders in the legend: Entisols and Inceptisols are slightly weathered; Mollisols, Alfisols, and Spodosols are intermediately weathered.

ratios for forest (0.25–0.6), agriculture (0.25–0.61), and developed (0.05–0.6) were consistent with the vertical patterns of P_{ox}.

DPS_{ox} was relatively constant at ≈ 10% throughout the 165 cm of wetland, the upper 120 cm of developed land, and the upper 200 cm of forest soils. This stable status of DPS_{ox} was altered at 125 cm for wetland soils and at 200 cm for forest soils, where DPS_{ox} started to increase with increasing depth and doubled (about 20%) at the bottom of the profiles. In contrast, DPS_{ox} was consistently more variable across the agricultural soil profiles and showed highest P loss risk in the upper 120 cm (Fig. S6E). The SPSC showed net P sources for the entire soil profiles under agriculture and wetlands and subsurface (30–200 cm) of developed soils. Net P sinks appeared in the upper 200 cm of forest soils and the upper 30 cm of developed lands (Fig. S6F).

3.4. Influence of environmental factors on vertical P distributions in streambanks

The effects of environmental factors on streambank P variables were depth-dependent within the upper 120 cm (Table 2). With increasing soil depth, the effect of riparian land cover on P_{tot} concentration decreased, while the influences of bedrock type and soil order on P_{tot} concentration increased. In the top 30 cm, specifically, riparian land cover had a strong influence on P_{tot} concentration (eta2[H] = 0.14, $p < 0.0001$) whereas the influences of bedrock type (eta2[H] = 0.08–0.1) and soil order (eta2[H] = 0.1–0.12) were moderate. At 45–120 cm, P_{tot} concentration had high dependence on bedrock (eta2[H] = 0.14–0.22) and soil order (eta2[H] = 0.14–0.22) compared to the moderate to small

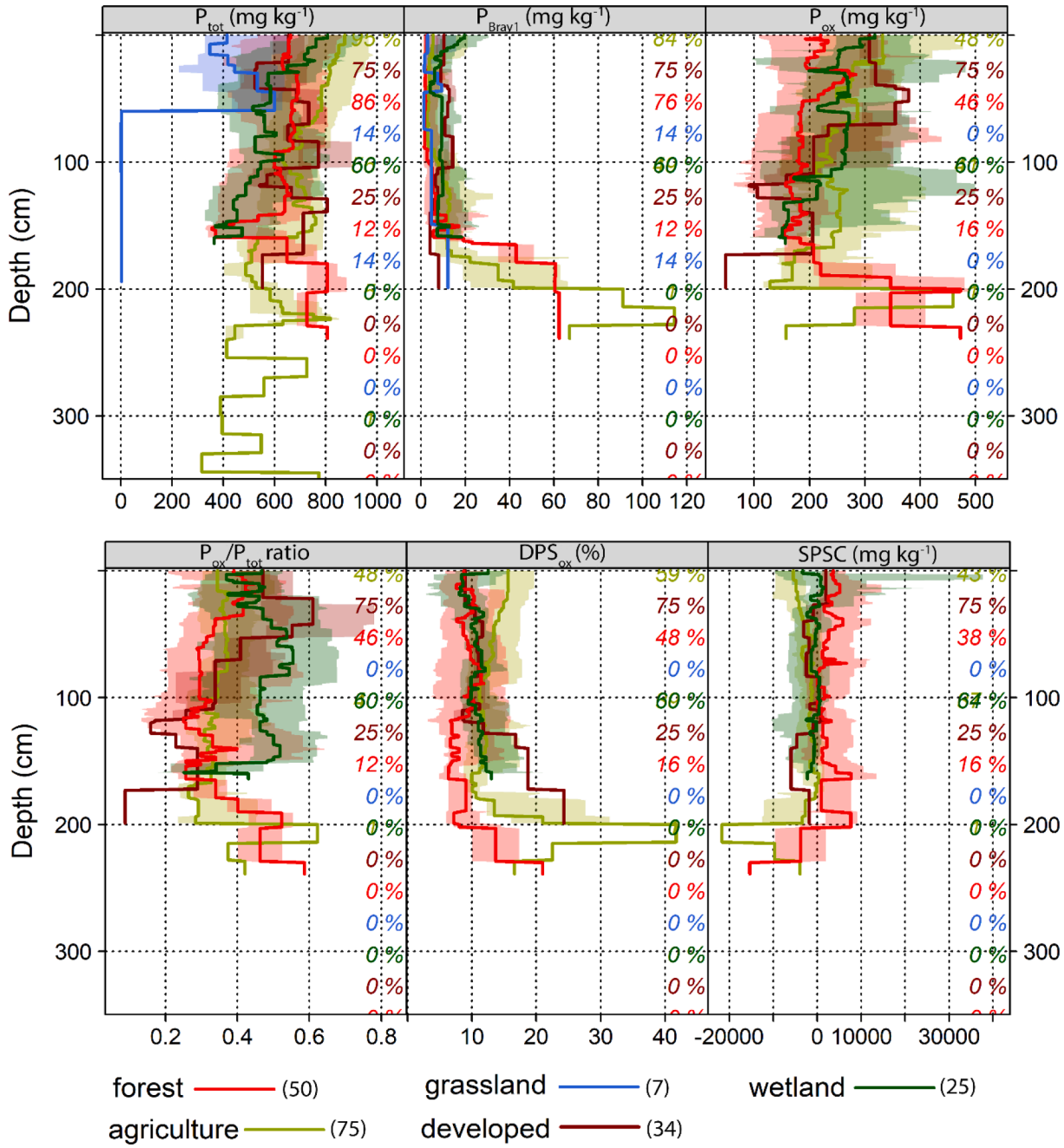

Fig. 4. Vertical profiles of P_{tot}, P_{Bray1}, P_{ox}, P_{ox}/P_{tot} ratios, DPS_{ox}, and SPSC in streambanks by riparian land covers. Solid lines are median values bounded by the interval defined by the 25th and 75th percentiles. Parentheses after the land cover name show the total number of soil profiles for each land use type. Values along the right-hand side y-axis describe the proportion of total profile observations with values reported at a given depth.

dependence on land cover (eta2[H] = 0.01–0.07). The effects of climate region (moderate) and parent material (small) on P_{tot} were relatively stable across the upper 120 cm depth. Riparian land cover was also found to greatly influence the P loss risk indices of DPS_{ox} and SPSC within the upper 30 cm.

3.5. Correlation between streambank P and soil properties

In addition to environmental factors, streambank P was affected differently by soil's physical and chemical properties (Fig. 5). P_{tot} and P_{ox} concentrations were negatively correlated with sand content and positively correlated with silt, clay, C_{tot}, CEC, Fe_{ox}, Al_{ox}, and Fe_{tot} content. P_{Bray1} was negatively correlated with clay/Fe_{ox} content and pH but unrelated to other soil properties. The P_{ox}/P_{tot} ratios were positively correlated with silt, clay, C_{tot}, CEC, Fe_{ox}, and Al_{ox} content and negatively correlated with sand content and pH. DPS_{ox} was weakly and negatively (R = -0.32) correlated with Fe_{ox} content; no significant correlations were found between DPS_{ox} and other soil properties. Similarly, SPSC was weakly and positively correlated with sand and Fe_{ox} content and weakly and negatively correlated with silt and Ca_{tot} content. Strong relationships were observed among the six streambank P variables, particularly between P_{tot} and P_{ox} (R = 0.77), P_{ox} and P_{ox}/P_{tot} ratios (R = 0.65).

4. Discussion

4.1. General trend and measurement gaps

The dataset used in this study represents the most comprehensive

Table 2
Standard effect size of environmental factors on total P (P_{tot}), Bray-1P (P_{Bray1}), oxalate-extractable P (P_{ox}), P_{ox}/P_{tot} ratio, degree of P saturation (DPS_{ox}), and soil P storage capacity (SPSC) by 15-cm depth intervals to 120 cm depth among streambank profiles. The eta squared based on the H-statistic (eta2[h]) were generated from the Kruskal-Wallis test at each depth interval with either P_{tot}, P_{Bray1}, P_{ox}, P_{ox}/P_{tot} ratio, DPS_{ox}, and SPSC as the responsible variables. An eta2[H] > 0.14 (bolded) is considered a large effect size, 0.06–0.14 moderate effect size (underlined), and < 0.06 low effect size.

Depth	Factor	eta2[H] index					
		P_{tot}	P_{Bray1}	P_{ox}	P_{ox}/P_{tot} ratio	DPS_{ox}	SPSC
0–15 cm	Climate region	*0.11*	0.05	−0.01	0.00	0.03	0.02
	Parent material	0.06	0.00	0.03	0.00	0.03	0.01
	Bedrock	*0.08*	0.04	−0.02	0.00	*0.07*	0.04
	Soil order	*0.12*	0.01	0.04	0.03	*0.13*	*0.09*
	Land cover	**0.14**	0.06	0.03	−0.01	**0.16**	**0.15**
	Sample size	142	134	79	79	90	71
15–30 cm	Climate region	*0.10*	0.01	0.00	0.01	0.05	0.02
	Parent material	0.05	−0.01	0.02	0.00	0.06	0.04
	Bedrock	*0.10*	0.04	−0.02	−0.01	*0.08*	0.02
	Soil order	*0.10*	0.01	0.03	0.00	0.04	0.01
	Land cover	**0.14**	0.03	0.02	0.00	**0.15**	**0.16**
	Sample size	144	135	80	80	94	71
30–45 cm	Climate region	*0.09*	−0.01	0.02	0.00	0.02	0.03
	Parent material	*0.07*	0.00	0.02	0.03	0.06	0.03
	Bedrock	*0.13*	0.01	0.00	−0.02	*0.07*	0.02
	Soil order	*0.11*	0.02	0.03	0.01	0.02	0.00
	Land cover	*0.09*	0.01	0.00	0.01	*0.08*	*0.08*
	Sample size	139	121	80	80	89	71
45–60 cm	Climate region	*0.09*	−0.02	0.02	0.00	0.04	0.04
	Parent material	0.06	0.01	0.02	0.02	0.06	0.04
	Bedrock	**0.19**	0.01	0.00	−0.01	0.04	0.01
	Soil order	**0.14**	0.02	0.03	0.01	0.01	0.00
	Land cover	*0.07*	0.04	0.02	0.01	0.03	0.04
	Sample size	138	124	80	79	89	71
60–75 cm	Climate region	*0.08*	−0.02	0.01	0.00	0.02	0.02
	Parent material	0.06	0.02	0.04	0.03	0.06	0.05
	Bedrock	**0.22**	0.01	0.00	0.00	−0.01	−0.01
	Soil order	**0.22**	0.03	0.04	0.02	0.01	0.01
	Land cover	0.04	0.06	0.00	0.01	0.01	0.02
	Sample size	131	122	80	79	82	71
75–90 cm	Climate region	0.04	−0.02	0.01	0.00	0.01	0.01
	Parent material	0.05	0.00	0.04	0.03	0.06	0.05
	Bedrock	**0.14**	0.01	0.01	0.03	−0.02	−0.01
	Soil order	**0.17**	0.03	0.03	0.02	0.02	0.02
	Land cover	0.01	0.04	−0.01	0.01	0.00	0.00
	Sample size	127	116	77	76	79	68
90–105 cm	Climate region	0.04	0.00	0.00	0.00	0.01	0.00
	Parent material	0.03	0.03	0.04	0.02	0.05	0.04
	Bedrock	0.02	0.01	−0.01	0.01	−0.02	−0.02
	Soil order	0.05	0.02	0.02	0.03	0.04	0.01
	Land cover	0.01	−0.01	0.00	0.00	0.00	0.01
	Sample size	96	88	77	75	70	69
105–120 cm	Climate region	0.04	0.00	−0.01	−0.01	0.01	0.01
	Parent material	−0.01	0.05	0.04	0.03	0.03	0.02
	Bedrock	0.04	0.03	−0.01	0.01	−0.02	−0.02
	Soil order	*0.09*	0.01	0.04	0.03	0.03	0.01
	Land cover	0.01	0.00	0.01	0.03	0.00	0.02
	Sample size	77	70	69	67	65	64
All depth	Climate region	*0.09*	0.00	0.01	0.01	0.03	0.03
	Parent material	*0.07*	0.02	0.05	0.03	*0.07*	0.06
	Bedrock	*0.12*	0.03	0.00	0.01	0.03	0.01
	Soil order	*0.13*	0.03	0.05	0.03	0.04	0.02
	Land cover	*0.06*	0.04	0.02	0.01	*0.06*	*0.07*

assessment of vertical P variations in streambanks, fusing soil profiles obtained by a systemic review of international scientific literature with USDA-NCSS pedon data. Some of the streambanks sampled by NCSS may not necessarily be subject to bank erosion problems. However, the inclusion of the NCSS dataset maximized the comprehensiveness of the metadata by providing additional climate regimes, parent material, bedrock types, soil types, and land covers. Therefore, this *meta*-dataset provides one of the most complete and up-to-date compilations for studying vertical P variation within the critical interface of streambanks at the pedon scale and for identifying drivers that explain P load and release potential to surface water by bank erosion.

However, this dataset is biased toward US conditions, which is probably due to local bank erosion severity (Manuel, 2014), high stream water P levels (Mekonnen and Hoekstra, 2018), and local regulatory efforts (USEPA, 2020). Compared to the US, the vertical distribution of streambank P in other countries has received less attention, with limited observations from Denmark, Nigeria, and Brazil. Though several studies have reported streambank P concentrations or loads in the UK (Ashbridge, 1995; Bull, 1997; Granger et al., 2021), New Zealand (Alexander et al., 2002; Sharpley and Syers, 1979), and Canada (Michaud et al., 2019; Rondeau et al., 2000), these studies were limited to soil P at surface depth. Generally, we find that existing studies of vertical P distribution in streambanks tend to focus on upper banks with depth of sampling that were shallower (mean 125 cm) than streambank height (mean 250 cm), indicating that deeper streambank P is being overlooked. Given the high variability of soil P concentrations across a bank

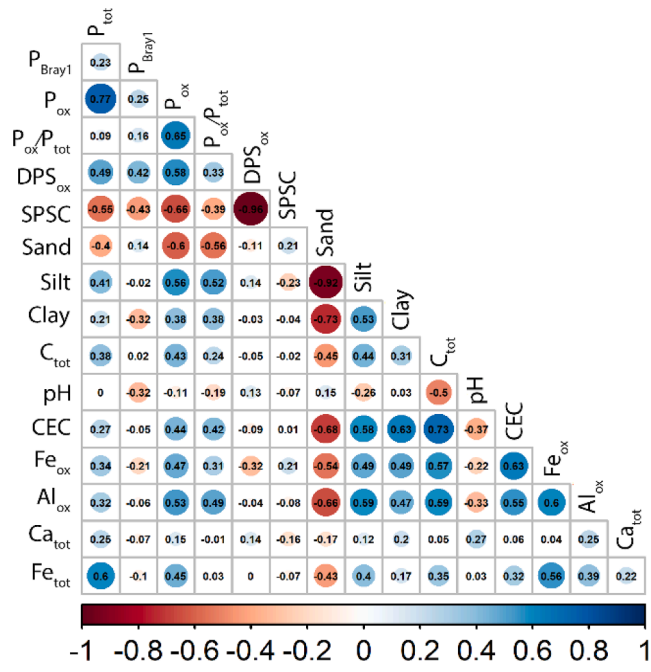

Fig. 5. Spearman correlation matrix of predictor variables related to soil P variables. A larger circle represents stronger correlations and color indicates the directionality of the correlation.

profile confirmed by our analysis, it is important to quantify deeper soil P levels in streambanks. In addition, quantifying deeper streambank P is helpful for more accurate estimates of P load from eroding banks as lower banks can experience significant amounts of soil and P loss from seepage undercuts and fluvial erosion (Fox and Wilson, 2010; Midgley et al., 2013). Though most soil profiles used in this study meet the standardize minimum pedon depth of 100 cm, we suggest that future evaluations of streambank soil P should standard sampling to encompass at least the full bank height from the water level, and ideally from the streambed level.

In addition to the overlooked deeper soil P, only 13% of the observations reported water-extractable P (P_w), resulting in insufficient data size to assess the stratification of this P fraction. P_w is useful in linking streambank erosion to downstream dissolved-reactive P (DRP) loads as it can rapidly enter the stream water as DRP upon erosion. Soil P_w was shown moderate to strong positive correlations (R^2 = 0.65–0.97) with surface runoff DRP (Kleinman et al., 2002; McDowell and Sharpley, 2001; Pote et al., 1999). Therefore, we suggest that soil P_w concentration by depth should be measured in terms of streambank erosion studies. Moreover, other P fractions such as sequentially extracted fractions (Hedley et al., 1982; Nakayama et al., 2021) should be also measured by depth as they can provide important insights into the fate of eroded sediment P. For example, iron-P vs. calcium-P pools inferred by sequential fractionation have different P dissolution dynamics under prolonged saturation (Reddy et al., 1999) that can help understand the fate of streambank soil P when eroded into stream channels.

4.2. Major drivers of streambank P vary by depth

Our analysis showed that riparian land cover, soil order, and bedrock type are major drivers of soil P_{tot} in streambanks and that the degree of their influences depends on soil depth. The predominant control of riparian land cover on P_{tot}, DPS_{ox}, and SPSC in surface soil is due to P inputs via manure, plant residue, and fertilizer, and P output via plant uptake, demonstrating the importance of vegetation and agricultural activities on soil P status and loss risks (Dzombak and Sheldon, 2020; Tufekcioglu, 2006). In the subsurface, however, the dominant role of soil order and bedrock type on P_{tot} over land cover likely reflects the geochemical processes on total P entailed by weathering and associated soil formation processes (Cross and Schlesinger, 1995; Walker and Syers, 1976). In particular, the large effect of bedrock on P_{tot} supports the hypothesized influence of bedrock P on soil P content (Porder and Ramachandran, 2013) (Fig. S7). In an apparent contradiction, however, we found a moderate to small influence of parent material on P_{tot}. This could be reconciled by the level of specificity in bedrock vs. parent material classification: "alluvial" parent material is broad and can encompass high mineralogical diversity, whereas bedrock provides a more site-specific P metric related to soils in the watershed. Since a large proportion of the streambank soils developed on stream-transported (77%) or ice-transported (10%) material, bedrock type could more specifically reflect parent material P content derived from upstream erosion than the broader classification of alluvium. The generally moderate influence of climate regions on P_{tot} across soil depths reflects general impact of this soil-forming factor on P status (Delgado-Baquerizo et al., 2020; Jenny, 1994).

Overall, trends in streambank P variables with depth were broadly consistent with major types and differences in horizons among soil orders, supporting the value of pedologically informed approaches to understanding vertical P distribution in streambanks. The amount of soil P depends on the relative age of soils that results from varying durations and intensities of weathering as partly captured by orders in USDA Soil Taxonomy (Boitt, 2017; Cross and Schlesinger, 1995; Jenny, 1994; Turner and Condron, 2013; Walker and Syers, 1976). That P_{tot} concentration generally decreased from minimally weathered Entisols to more weathered Alfisols and Spodosols is consistent with relative differences in P_{tot} among these soil orders reported by other researchers (Dzombak and Sheldon, 2020; Yang and Post, 2011). The highest P_{tot} occurring at the top streambank likely reflects surface P accumulation via litter deposition (Fenton, 1983). However, the P trend in the subsurface is challenging to interpret given the potential interactions between pedologic weathering and alluvial processes of subsurface soil. The irregular increase in P_{tot} at 200 to 240 cm of Entisols and Inceptisols could be due to buried A horizons by alluvial deposits (Boettinger, 2005), as Entisols and Inceptisols are often formed on alluvium and commonly occur along river corridors (Foss et al., 1983; Grossman, 1983). Higher P_{ox}/P_{tot} ratios and DPS_{ox} in the subsurface of Entisols and Inceptisols are due to increased P_{ox} concentrations. Since P_{ox} is a good indicator of desorbable P (Maguire et al., 2000) and P availability in noncalcareous soils (Koopmans et al., 2004), these results collectively indicate that deep soil labile P from the lower bank, not just surface P, should be also considered in bank P assessments. The elevated P_{tot} between 15 and 30 cm of Mollisols could be due to organic P accumulation derived from roots in the subsurface (Fenton, 1983). P_{tot} of Alfisols was uniformly higher near the surface, decreased to a minimum between 20 and 25 cm, increased to a maximum from 50 to 105 cm, which could be due to P accumulation in the high clay B horizon that is characteristic of this soil type (Rust, 1983). It is worth noting Spodosols and Alfisols had similar vertical patterns of P, potentially mirroring the marked horizon differentiation of P-enriched O and B horizons separated by a P-poor E horizon (McKeague et al., 1983).

Although most of the streambank soils in this *meta*-dataset were relatively low in P_{Bray1} (critical value for most crops range 12–21 mg kg^{-1}) (Dodd and Mallarino, 2005), P_{tot} and P_{ox} suggest the P-enriching influence of agricultural (cultivated crops, hay, pasture) and urban land uses on streambank soil P. Though pair-wise comparisons for non-agricultural versus non-urban for each specific site were not conducted in this study, this still offers a useful survey and is consistent with reported impacts of land uses on soil P (Dzombak and Sheldon, 2020; Perillo et al., 2019). Streambanks adjacent to these two lands with potential anthropogenic P inputs (fertilizer, manure, waste) had higher mean P_{tot} and P_{ox} concentrations than the streambanks of non-agricultural or non-urban land uses, particularly in the upper 75 cm (Fig. S6A, 6C). Though streambanks are unlikely to be directly fertilized,

adsorption of DRP in surface runoff or deposition of P-rich soil particles transported from adjacent farmland can lead to soil P enrichment in surface soils of streambanks (Perillo et al., 2019). This P enrichment could explain the high P loss risk (Fig. S6E) and net P sources in banks with agricultural lands (Fig. S6F). Adsorption of DRP from groundwater could be another contributing source of P to streambank soil P loads (Holman et al., 2008; Thompson and McFarland, 2010).

Independent of anthropogenic inputs, vegetation-specific organic matter can contribute to soil P_{tot} (Jenny, 1994). As P is a constituent of organic matter (Dalal, 1977; Turner et al., 2005), organic matter accumulation in surface soils may partially explain the higher P_{tot}, P_{Bray1}, and P_{ox} in the top 50 cm of banks with wetlands, forests, and grassland. Specifically, the relatively high P_{tot} in banks associated with wetlands could be attributed to faster organic matter storage under anaerobic conditions (Huang et al., 2015; Rejmánková and Houdková, 2006). In contrast, P_{tot} concentration in streambanks with forests was in lower values and less variant in the upper 150 cm, which could be due to interacting surface P leaching and root uptake of subsurface P (Zhang et al., 2021).

4.3. *Linking vertical P distribution in streambanks to pedogenic and fluvial histories*

The potential coexistence of pedogenic weathering and fluvial processes demonstrates the necessity of integrating soil science and hydrology to study vertical P distribution in streambanks. The five soil orders (Entisols, Inceptisols, Mollisols, Alfisols, and Spodosols) identified in this study were commonly developed along stream corridors on unconsolidated fluvial sediments with small portions developed on glaciolacustrine, glacial till, and loess material. This is illustrated by four HUC-10 example watersheds involved in this *meta*-dataset (Fig. 6), in which soil orders mapped along the river corridors depart from the watershed-dominant soil orders and occupy the second largest area of the watersheds: Inceptisols along Mad River (Fig. 6A), Alfisols along Spavinaw Creek (Fig. 6B), Entisols along Clark Run (Fig. 6C) and Jwett Creek (Fig. 6D). In this *meta*-analysis, the less developed (and thus coarser textured) Entisols (24%) and Inceptisols (60%) account for large proportions of the soil types, indicating the concerted influence of fluvial erosion and deposition processes with weathering processes on streambank soils. Soils on streambanks may be formed by weathering of local bedrock and/or from eroded and deposited alluvial material through fluvial processes (Fox et al., 2016), shaping distinct P distribution in streambanks with depth (compared to upland soils).

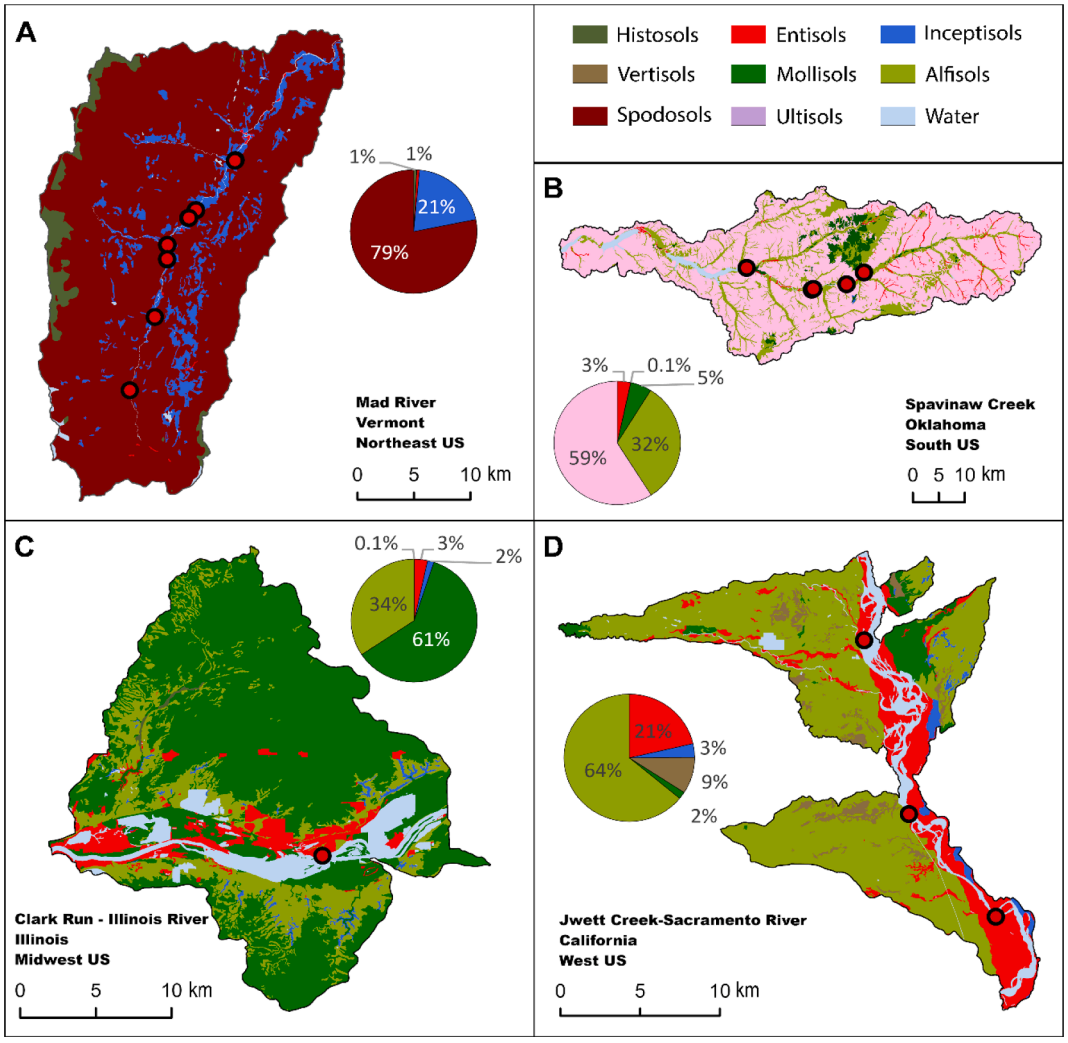

Fig. 6. Spatial distribution of soil orders in four HUC-10 watersheds representing the four regions of the US: (A) Mad River in Vermont, northeast US, (B) Spavinaw Creek in Oklahoma, south US, (C) Clark Run at Illinois River in Illinois, Midwestern US, (D) Jwett Creek at Sacramento River in California, west US. Red dots are soil profile locations. The pie charts show the percentage of soil orders by area. The water area is excluded from the pie charts to depict the relative proportion of soil orders.

To illustrate these interacting processes, Fig. 7B conceptualizes a typical cross-section of a meander bend (Fig. 7A) from the outer cut bank to the inner depositional bank (i.e., point bar). Sediment and P are transported into streams from the cut bank and deposited in the inner bank as point bars (Gillespie et al., 2018; Naito and Parker, 2019; Page and Nanson, 1982). Here, we focus on the vertical P characteristics on the outer cut banks that undergo net P loss from erosion. Initially, the foundation of the cut bank may consist of horizons formed from pedogenic processes, with P_{tot} vertical distribution expected to reflect soil formation by weathering processes such as illuviation (Eger et al., 2018). However, overbank flow during flood events can deposit large amounts of alluvium that bury the streambank soil (Naito and Parker, 2019). Large flood events (e.g., 100-year event) with long return periods (Deraman et al., 2017) may allow for the development of A horizons but is likely insufficient for the development of a B horizon(s) in most climates. During the second overbank deposition event, the first A horizon is buried by new alluvial sediments based on which the second A horizon will form as vegetation colonizes the bank surface; this process may repeat multiple times. Therefore, the quantity and distribution of soil P in streambanks not only provide a useful index for understanding pedogenetic processes (Smeck, 1973) or relative age of soils (Walker and Syers, 1976) but also offer valuable insights for decoding streambank erosion and deposition histories to better estimate P budgets in watersheds.

4.4. Limitations and implications

A potential limitation of this *meta*-analysis is that 95% of the observations were from the US with no observations from Asia or Australia, though this serves to highlight the research gap on streambank P profiles in other regions of the world. Nonetheless, the present *meta*-dataset appears to be the most comprehensive to date on streambank soil P profiles, with a wide range of stream orders, climate regimes, parent material, soil orders, and riparian land covers. A second potential weakness is that the fixed-depth approach used by many studies in reporting soil P likely entails merging horizons, which can challenge the interpretation of the vertical distribution of P variables based on pedogenic processes. On the other hand, fixed-depth reporting of soil data is not uncommon (Ishee et al., 2015; Odhiambo et al., 2016; Schilling et al., 2009; Veihe et al., 2011). Future streambank soil assessments that consider genetic horizons may offer greater interpretative power. We also suggest that future studies report measures of P forms, such as P_w

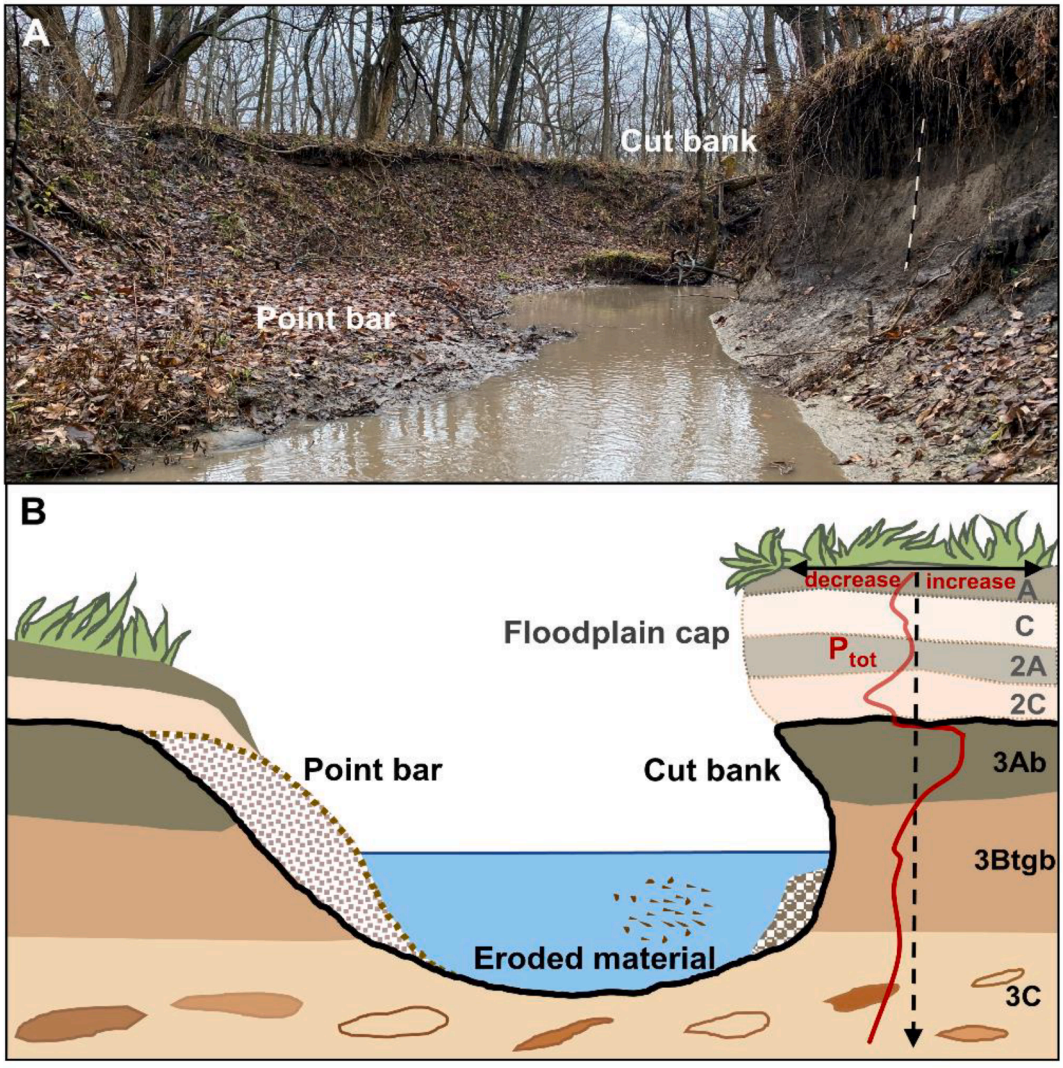

Fig. 7. (A) A meander bend of Polecat Creek, IL, US. Each interval of black-and-white profile marker in the foreground of the right-hand side of the photo (i.e., cut bank) is 10 cm. (B) a conceptual depiction of the meander bend reflecting soil-formation and erosion–deposition histories (based in part on Naito and Parker (2019)), as well as variation of total P (P_{tot}) concentration with depth in the cut bank profile. Note that the floodplain cap (color faded) on top of the cut bank would not be present for banks that have not experienced overbank deposition events.

and sequentially extracted P fractions, given that they can differ in fate upon mobilization into streams. Finally, paired monitoring of streambank soil P profiles and neighboring stream water P at short time intervals are needed to link deeper soil P with P load from eroding banks and improve the accuracy of estimating streambank contribution to watershed P export.

5. Conclusions

Soil P concentration in streambanks is crucial for accurately estimating P load to streams via bank erosion, but often lacks detailed examination. In contrast to upland soils, variation of streambank P with depth is likely to be affected in concert by weathering processes and concomitant erosion and depositional processes. Using a *meta*-dataset encompassing a wide range of climatic contexts, this work systemically assessed the vertical distribution of total P (P_{tot}), forms of P (P_{Bray1} and P_{ox}), and environmental P loss risks (DPS_{ox} and SPSC) in streambanks with various soil types and riparian land covers worldwide. Our analysis identified that studies to date generally used insufficient soil sampling depth relative to bank height and do not commonly measure P fractions that correspond to P species of likely differing fate upon transportation into streams. The depth distribution patterns of P_{tot} are broadly consistent with major differences in horizons among soil orders, suggesting the value of broad pedogenic concepts to understand vertical P distribution in streambank soils. The degree of influence of environmental factors on streambank P is depth-dependent. The riparian land cover had a large influence on surface soil P (top 30 cm), whereas soil order and bedrock type had large influences on subsurface P. Streambanks proximate to agricultural land had significantly higher P_{tot} and P loss risk in the upper 60 cm than other land covers. The soils were largely alluvium derived Entisols (24%) and Inceptisols (60%) and demonstrate the importance of considering fluvial erosion–deposition induced alluvial stratification on the vertical distribution of streambank P. To improve understanding of streambank erosion and P loading, an integrated pedo-hydrologic assessment of soil P in streambanks is needed and the interactions of weathering, fluvial erosion and deposition, and riparian land cover should be considered. This work helps advance the fundamental understanding of soil P transfers at the terrestrial-aquatic interface of streambanks by integrating soil science and stream hydrology and highlights the need for quantifying deep soil total P and P fractions in streambanks to better characterize soil P pools and environmental P risk upon bank erosion.

6. Research data

All associated data and code will be shared upon request.

Declaration of Competing Interest

The authors declare that they have no known competing financial interests or personal relationships that could have appeared to influence the work reported in this paper.

Acknowledgments

This research was supported by the Illinois Nutrient Research and Education Council (NREC) 2021-4-360731-469. We thank Yuhei Nakayama for providing advice on systematic literature review methodology in the early stages of manuscript development. We thank the two anonymous reviewers for their comments and suggestions that helped to improve the quality of this manuscript.

Appendix A. Supplementary data

Supplementary data to this article can be found online at https://doi.org/10.1016/j.geoderma.2022.115989.

References

Abdala, D.B., da Silva, I.R., Vergütz, L., Sparks, D.L., 2015. Long-term manure application effects on phosphorus speciation, kinetics and distribution in highly weathered agricultural soils. Chemosphere 119, 504–514.
Ahern, C.R., Baker, D.E., Aitken, R.L., 1995. Models for relating pH measurements in water and calcium chloride for a wide range of pH, soil types and depths. Springer, Netherlands, pp. 99–104.
Alexander, R.B., Elliott, A.H., Shankar, U., McBride, G.B., 2002. Estimating the sources and transport of nutrients in the Waikato River Basin, New Zealand. Water Resour. Res. 38 (12), 4-1–4-23.
Ashbridge, D., 1995. Processes of river bank erosion and their contribution to the suspended sediment load of the River Culm, Devon. Sediment and water quality in river catchments 229–245.
Beaudette, D., Roudier, P., Brown, A., 2021. aqp: Algorithms for Quantitative Pedology. R package version 1.31., https://CRAN.R-project.org/package=aqp.
Beck, W., Isenhart, T., Moore, P., Schilling, K., Schultz, R., Tomer, M., 2018. Streambank Alluvial Unit Contributions to Suspended Sediment and Total Phosphorus Loads, Walnut Creek, Iowa, USA. Water 10 (2), 111.
Bockheim, J.G., Gennadiyev, A.N., Hartemink, A.E., Brevik, E.C., 2014. Soil-forming factors and Soil Taxonomy. Geoderma 226–227, 231–237.
Boettinger, J.L., 2005. Alluvium and alluvial soils. In: Hillel, D. (Ed.), Encyclopedia of Soils in the Environment. Elsevier, Oxford, pp. 45–49.
Boitt, G., 2017. Phosphorus legacy: role of long-term soil phosphorus accumulation in the sustainable management of intensive agroecosystems, Lincoln University.
Bray, R.H., Kurtz, L.T., 1945. Determination of total, organic, and available forms of phosphorus in soils. Soil Sci. 59 (1), 39–46.
Bull, L.J., 1997. Magnitude and variation in the contribution of bank erosion to the suspended sediment load of the River Severn. UK. Earth Surface Processes and Landforms 22 (12), 1109–1123.
Chai, H., Yu, G., He, N., Wen, D., Li, J., Fang, J., 2015. Vertical distribution of soil carbon, nitrogen, and phosphorus in typical Chinese terrestrial ecosystems. Chinese Geographical Science 25 (5), 549–560.
Cross, A.F., Schlesinger, W.H., 1995. A literature review and evaluation of the. Hedley fractionation: Applications to the biogeochemical cycle of soil phosphorus in natural ecosystems. Geoderma 64 (3–4), 197–214.
Culman, S., Mann, M., Sharma, S., Saeed, M., Fulford, A., Lindsey, L., Joern, B., 2019. Converting between Mehlich-3, Bray P, and ammonium acetate soil test values. The Ohio State University, Ohio.
Dalal, R.C., 1977. Soil Organic Phosphorus. Elsevier 83–117.
Delgado-Baquerizo, M., Reich, P.B., Bardgett, R.D., Eldridge, D.J., Lambers, H., Wardle, D.A., Reed, S.C., Plaza, C., Png, G.K., Neuhauser, S., Berhe, A.A., Hart, S.C., Hu, H.-W., He, J.-Z., Bastida, F., Abades, S., Alfaro, F.D., Cutler, N.A., Gallardo, A., García-Velázquez, L., Hayes, P.E., Hseu, Z.-Y., Pérez, C.A., Santos, F., Siebe, C., Trivedi, P., Sullivan, B.W., Weber-Grullon, L., Williams, M.A., Fierer, N., 2020. The influence of soil age on ecosystem structure and function across biomes. Nat. Commun. 11 (1), 4721.
DeWolfe, N.M., Hession, W.C., Watzin, C.M., 2004. Sediment and Phosphorus Loads from Streambank Erosion in Vermont, USA.
Deraman, W.H.A., Abd Mutalib, N.J., Mukhtar, N.Z., 2017. Determination of return period for flood frequency analysis using normal and related distributions. J. Phys. Conf. Ser. IOP Publishing 890, 012162.
Dodd, J.R., Mallarino, A.P., 2005. Soil-Test Phosphorus and Crop Grain Yield Responses to Long-Term Phosphorus Fertilization for Corn-Soybean Rotations. Soil Sci. Soc. Am. J. 69 (4), 1118–1128.
Drevon, D., Fursa, S.R., Malcolm, A.L., 2017. Intercoder reliability and validity of WebPlotDigitizer in extracting graphed data. Behav. Modif. 41 (2), 323–339.
Dzombak, R.M., Sheldon, N.D., 2020. Weathering Intensity and Presence of Vegetation Are Key Controls on Soil Phosphorus Concentrations: Implications for Past and Future Terrestrial Ecosystems. Soil Systems 4 (4), 73.
Eger, A., Yoo, K., Almond, P.C., Boitt, G., Larsen, I.J., Condron, L.M., Wang, X., Mudd, S. M., 2018. Does soil erosion rejuvenate the soil phosphorus inventory? Geoderma 332, 45–59.
Fenton, T.E., 1983. Chapter 4 Mollisols. Elsevier, pp. 125-163.
Fick, S.E., Hijmans, R.J., 2017. WorldClim 2: new 1-km spatial resolution climate surfaces for global land areas. Int. J. Climatol. 37 (12), 4302–4315.
Foss, J.E., Moormann, F.R., Rieger, S., 1983. Chapter 10 Inceptisols. Elsevier, pp. 355-381.
Fox, G.A., Purvis, R.A., Penn, C.J., 2016. Streambanks: A net source of sediment and phosphorus to streams and rivers. J. Environ. Manage. 181, 602–614.
Fox, G.A., Wilson, G.V., 2010. The role of subsurface flow in hillslope and stream bank erosion: A Review. Soil Sci. Soc. Am. J. 74 (3), 717–733.
Gillespie, J.L., Noe, G.B., Hupp, C.R., Gellis, A.C., Schenk, E.R., 2018. Floodplain Trapping and Cycling Compared to Streambank Erosion of Sediment and Nutrients in an Agricultural Watershed. J. Am. Water Resour. Assoc. 54 (2), 565–582.
Granger, S.J., Harris, P., Upadhayay, H.R., Sint, H., Pulley, S., Stone, M., Krishnappan, B. G., Collins, A.L., 2021. Novel approaches to investigating spatial variability in channel bank total phosphorus at the catchment scale. CATENA 202, 105223.
Grossman, R.B., 1983. Chapter 2 Entisols. Elsevier, pp. 55-90.
Hedley, M.J., Stewart, J.W.B., Chauhan, B.S., 1982. Changes in inorganic and organic soil phosphorus fractions induced by cultivation practices and by laboratory incubations. Soil Sci. Soc. Am. J. 46 (5), 970–976.
Hoffmann, C.C., Kjaergaard, C., Uusi-Kämppä, J., Hansen, H.C.B., Kronvang, B., 2009. Phosphorus retention in riparian buffers: review of their efficiency. J. Environ. Qual. 38 (5), 1942–1955.

Holman, I.P., Whelan, M.J., Howden, N.J.K., Bellamy, P.H., Willby, N.J., Rivas-Casado, M., McConvey, P., 2008. Phosphorus in groundwater-an overlooked contributor to eutrophication? Hydrol. Process. 22 (26), 5121–5127.
Horton, J.D., 2017. The State Geologic Map Compilation (SGMC) geodatabase of the conterminous United States.
Houlahan, J.E., Findlay, C.S., 2004. Estimating the 'critical'distance at which adjacent land-use degrades wetland water and sediment quality. Landscape Ecol. 19 (6), 677–690.
Huang, W., Chen, Q., Ren, K., Chen, K., 2015. Vertical distribution and retention mechanism of nitrogen and phosphorus in soils with different macrophytes of a natural river mouth wetland. Environ. Monit. Assess. 187 (3).
Ishee, E.R., Ross, D.S., Garvey, K.M., Bourgault, R.R., Ford, C.R., 2015. Phosphorus characterization and contribution from eroding streambank soils of Vermont's Lake Champlain basin. J. Environ. Qual. 44 (6), 1745–1753.
Jenny, H., 1994. Factors of soil formation: a system of quantitative pedology. Courier Corporation.
Kessler, A.C., Gupta, S.C., Dolliver, H.A.S., Thoma, D.P., 2012. Lidar Quantification of Bank Erosion in Blue Earth County, Minnesota. J. Environ. Q. 41 (1), 197–207.
Ketterings, Q.M., Czymmek, K.J., Reid, W.S., Wildman, R.F., 2002. Conversion of modified morgan and mehlich-iii soil tests to morgan soil test values. Soil Sci. 167 (12), 830–837.
Kleinman, P.J.A., Sharpley, A.N., Wolf, A.M., Beegle, D.B., Moore, P.A., 2002. Measuring water-extractable phosphorus in manure as an indicator of phosphorus in runoff. Soil Sci. Soc. Am. J. 66 (6), 2009–2015.
Koopmans, G.F., Chardon, W.J., Ehlert, P.A.I., Dolfing, J., Suurs, R.A.A., Oenema, O., Van Riemsdijk, W.H., 2004. Phosphorus availability for plant uptake in a phosphorus-enriched noncalcareous sandy soil. J. Environ. Qual. 33 (3), 965.
Kronvang, B., Audet, J., Baattrup-Pedersen, A., Jensen, H.S., Larsen, S.E., 2012. Phosphorus load to surface water from bank erosion in a Danish lowland river basin. J. Environ. Qual. 41 (2), 304–313.
Kronvang, B., Grant, R., Laubel, A.L., 1997. Sediment and phosphorus export from a lowland catchment: Quantification of sources. Water Air Soil Pollut. 99 (1–4), 465–476.
Lambers, H., Barrow, N.J., 2020. Pervasive use of P 2 O 5, K 2 O, CaO, MgO, and basic cations, none of which exist in soil. Springer. 56 (6), 743–745.
Laubel, A., Kronvang, B., Hald, A.B., Jensen, C., 2003. Hydromorphological and biological factors influencing sediment and phosphorus loss via bank erosion in small lowland rural streams in Denmark. Hydrol. Process. 17 (17), 3443–3463.
Layzell, A.L., Mandel, R.D., 2014. An assessment of the erodibility of Holocene lithounits comprising streambanks in northeastern Kansas, USA. Geomorphology 213, 116–127.
MacDonald, G.K., Bennett, E.M., Potter, P.A., Ramankutty, N., 2011. Agronomic phosphorus imbalances across the world's croplands. Proc. Natl. Acad. Sci. 108 (7), 3086–3091.
Maguire, R., Sims, J., Coale, F., 2000. Phosphorus fractionation in biosolids-amended soils relationship to soluble and desorbable phosphorus. Soil Sci. Soc. Am. J. 64 (6), 2018–2024.
Mallarino, A.P., 1995. Comparison of Mehlich-3, Olsen, and Bray-P1 procedures for phosphorus in calcareous soils. The North Central Extension-Industry Soil Fertility Conference 11, 6.
Manuel, J., 2014. Nutrient pollution: A persistent threat to waterways. Environ. Health Perspect. 122 (11).
McDowell, R., Sharpley, A., 2001. Approximating phosphorus release from soils to surface runoff and subsurface drainage. J. Environ. Qual. 30 (2), 508–520.
McDowell, R., Sharpley, A., Folmar, G., 2001. Phosphorus export from an agricultural watershed: Linking source and transport mechanisms. J. Environ. Qual. 30 (5), 1587–1595.
McKeague, J.A., Deconinck, F., Franzmeier, D.P., 1983. Chapter 6 Spodosols. Elsevier, pp. 217-252.
Mekonnen, M.M., Hoekstra, A.Y., 2018. Global Anthropogenic Phosphorus Loads to Freshwater and Associated Grey Water Footprints and Water Pollution Levels: A High-Resolution Global Study. Water Resour. Res. 54 (1), 345–358.
Michaud, A.R., Poirier, S.C., Whalen, J.K., 2019. Tile drainage as a hydrologic pathway for phosphorus export from an agricultural subwatershed. J. Environ. Qual. 48 (1), 64–72.
Midgley, T.L., Fox, G.A., Wilson, G.V., Heeren, D.M., Langendoen, E.J., Simon, A., 2013. Seepage-induced streambank erosion and instability: In situ constant-head experiments. J. Hydrol. Eng. 18 (10), 1200–1210.
Moustakidis, I.V., Schilling, K.E., Weber, L.J., 2019. Soil total phosphorus deposition and variability patterns across the floodplains of an Iowa river. Catena 174, 84–94.
Nair, V., Harris, W., 2004. A capacity factor as an alternative to soil test phosphorus in phosphorus risk assessment. N. Z. J. Agric. Res. 47 (4), 491–497.
Nair, V.D., 2014. Soil phosphorus saturation ratio for risk assessment in land use systems. Front Env. Sci-Switz 2 (6).
Naito, K., Parker, G., 2019. Can bankfull discharge and bankfull channel characteristics of an alluvial meandering river be cospecified from a flow duration curve? J. Geophys. Res. Earth Surf. 124 (10), 2381–2401.
Nakayama, Y., Wade, J., Margenot, A.J., 2021. Does soil phosphomonoesterase activity reflect phosphorus pools estimated by Hedley phosphorus fractionation? Geoderma 401, 115279.
Nelson, N.O., Parsons, J.E., Mikkelsen, R.L., 2005. Field-scale evaluation of phosphorus leaching in acid sandy soils receiving swine waste. J. Environ. Qual. 34 (6), 2024–2035.
O'Geen, A., Walkinshaw, M., Beaudette, D., 2017. SoilWeb: A multifaceted interface to soil survey information. Soil Sci. Soc. Am. J. 81 (4), 853–862.
Odhiambo, B.K., Ricker, M.C., Le Blanc, L.M., Moxey, K.A., 2016. Effects of forested floodplain soil properties on phosphorous concentrations in two Chesapeake Bay sub-watersheds, Virginia, USA. Environ. Sci. Pollut. R 23 (16), 16056–16066.
Ogle, D.H., J.C. Doll, P. Wheeler, Dinno., A., 2021. 021. FSA: Fisheries Stock Analysis. R package version 0.9.1., https://github.com/droglenc/FSA.
Page, K., Nanson, G., 1982. Concave-bank benches and associated floodplain formation. Earth Surf. Proc. Land. 7 (6), 529–543.
Pai, N., Saraswat, D., 2013. A geospatial tool for delineating streambanks. Environ. Modell. Software 40, 151–159.
Peacher, R.D., Lerch, R.N., Schultz, R.C., Willett, C.D., Isenhart, T.M., 2018. Factors controlling streambank erosion and phosphorus loss in claypan watersheds. J. Soil Water Conserv. 73 (2), 189–199.
Perillo, V.L., Cade-Menun, B.J., Ivancic, M., Ross, D.S., Wemple, B.C., 2021. Land use and landscape position influence soil organic phosphorus speciation in a mixed land use watershed. J. Environ. Qual. 50 (4), 967–978.
Perillo, V.L., Ross, D.S., Wemple, B.C., Balling, C., Lemieux, L.E., 2019. Stream Corridor Soil Phosphorus Availability in a Forested-Agricultural Mixed Land Use Watershed. J. Environ. Qual. 48 (1), 185–192.
Porder, S., Ramachandran, S., 2013. The phosphorus concentration of common rocks—a potential driver of ecosystem P status. Plant Soil 367 (1–2), 41–55.
Pote, D.H., Daniel, T.C., Nichols, D.J., Sharpley, A.N., Moore, P.A., Miller, D.M., Edwards, D.R., 1999. Relationship between Phosphorus Levels in Three Ultisols and Phosphorus Concentrations in Runoff. J. Environ. Qual. 28 (1), 170–175.
Pradhan, S.N., Ghosh, A.K., Seema, Ram, S., Pal, Y., Pradhan, C., 2021. Changes in degree of phosphorus saturation and risk of P loss upon twelve years of manuring and reduced tillage. Geoderma 404, 115277.
Pribyl, D.W., 2010. A critical review of the conventional SOC to SOM conversion factor. Geoderma 156 (3–4), 75–83.
Purvis, R.A., Fox, G.A., Penn, C.J., Storm, D.E., Parnell, A., 2016. Estimating Streambank Phosphorus Loads at the Watershed Scale with Uncertainty Analysis Approach. J. Hydrol. Eng. 21 (9), 12.
R Core Team, 2021. R: A language and environment for statistical computing. R Foundation for Statistical Computing.
Reddy, K., Kadlec, R., Flaig, E., Gale, P., 1999. Phosphorus retention in streams and wetlands: a review. Critical Reviews in Environmental Science and Technology 29 (1), 83–146.
Rejmánková, E., Houdková, K., 2006. Wetland plant decomposition under different nutrient conditions: what is more important, litter quality or site quality? Biogeochemistry 80 (3), 245–262.
Rondeau, B., Cossa, D., Gagnon, P., Bilodeau, L., 2000. Budget and sources of suspended sediment transported in the St. Lawrence River, Canada. Hydrol. Process. 14 (1), 21–36.
Rowe, H., Withers, P.J.A., Baas, P., Chan, N.I., Doody, D., Holiman, J., Jacobs, B., Li, H. G., MacDonald, G.K., McDowell, R., Sharpley, A.N., Shen, J.B., Taheri, W., Wallenstein, M., Weintraub, M.N., 2016. Integrating legacy soil phosphorus into sustainable nutrient management strategies for future food, bioenergy and water security. Nutr. Cycl. Agroecosyst. 104 (3), 393–412.
Rust, R.H., 1983. Chapter 7 Alfisols. Elsevier, pp. 253-281.
Sayre, R., Karagulle, D., Frye, C., Boucher, T., Wolff, N.H., Breyer, S., Wright, D., Martin, M., Butler, K., Van Graafeiland, K., Touval, J., Sotomayor, L., McGowan, J., Game, E.T., Possingham, H., 2020. An assessment of the representation of ecosystems in global protected areas using new maps of World Climate Regions and World Ecosystems. Global Ecol. Conserv. 21, e00860.
Schilling, K.E., Isenhart, T.M., Wolter, C.F., Streeter, M.T., Kovar, J.L., 2021. Contribution of streambanks to phosphorus export from Iowa. Journal of Soil and Water 77 (2), 103–112.
Schilling, K.E., Palmer, J.A., Bettis, E.A., Jacobson, P., Schultz, R.C., Isenhart, T.M., 2009. Vertical distribution of total carbon, nitrogen and phosphorus in riparian soils of Walnut Creek, southern Iowa. CATENA 77 (3), 266–273.
Sharpley, A., Jarvie, H.P., Buda, A., May, L., Spears, B., Kleinman, P., 2013. Phosphorus Legacy: Overcoming the Effects of Past Management Practices to Mitigate Future Water Quality Impairment. J. Environ. Qual. 42 (5), 1308–1326.
Sharpley, A.N., Syers, J.K., 1979. Phosphorus inputs into a stream draining an agricultural watershed. Water Air Soil Pollut. 11 (4), 417–428.
Smeck, N.E., 1973. Phosphorus: an indicator of pedogenetic weathering processes. Soil Sci. 115 (3), 199–206.
Stackpoole, S.M., Stets, E.G., Sprague, L.A., 2019. Variable impacts of contemporary versus legacy agricultural phosphorus on US river water quality. P. Natl. Acad. Sci. U.S.A. 116 (41), 20562–20567.
Staff, S.S., 1999. Soil taxonomy: A basic system of soil classification for making and interpreting soil surveys, U.S. Department of Agriculture Handbook 436, 2nd edition ed. Natural Resources Conservation Service.
Staff, S.S., Service, N.R.C., Agriculture, U.S.D.o., 2021. Web Soil Survey, https://websoilsurvey.nrcs.usda.gov/.
Stott, D., 2019. Recommended soil health indicators and associated laboratory procedures. Soil Health Technical Note.
Strahler, A., 1957. Quantitative analysis of watershed geomorphology. American Geophysical Union Transactions 38, 913–920.
Suchet, P.A., Probst, J.L., Ludwig, W., 2003. Worldwide distribution of continental rock lithology: Implications for the atmospheric/soil CO2 uptake by continental weathering and alkalinity river transport to the oceans. Global Biogeochem Cy 17 (2).
Terence, C.B., 1987. Sedimentary Processes, Vertical Stratification Sequences, and Geomorphology of the Roaring River Alluvial Fan, Rocky Mountain National Park. Colorado. SEPM Journal of Sedimentary Research 57.

Thompson, C.A., McFarland, A.M.S., 2010. Effects of Surface and Groundwater Interactions on Phosphorus Transport within Streambank Sediments. J. Environ. Qual. 39 (2), 548–557.
Tiessen, H., Stewart, J.W., 1985. The biogeochemistry of soil phosphorus. Planetary ecology 463–472.
Tomczak, M., Tomczak, E., 2014. The need to report effect size estimates revisited. An overview of some recommended measures of effect size. Trends in Sport Sciences 1 (21), 19–25.
Tran, T.S., N'dayegamiye, A., 1995. Long-term effects of fertilizers and manure application on the forms and availability of soil phosphorus. Can. J. Soil Sci. 75 (3), 281–285.
Tufekcioglu, M., 2006. Riparian land-use impacts on stream bank soil and phosphorus losses from grazed pastures.
Tufekcioglu, M., 2010. Stream bank soil and phosphorus losses within grazed pasture stream reaches in the Rathbun Watershed in southern Iowa.
Turner, B.L., Condron, L.M., 2013. Pedogenesis, nutrient dynamics, and ecosystem development: the legacy of T.W. Walker and J.K. Syers. Plant Soil 367 (1-2), 1–10.
Turner, B.L., Frossard, E., Baldwin, D.S., 2005. Organic phosphorus in the environment. CABI Pub.
USEPA, 2020. National Rivers and Streams Assessment 2013-2014: Collaborative Survey. EPA 841-R-19-001. Washington, DC.
Veihe, A., Jensen, N.H., Schiotz, I.G., Nielsen, S.L., 2011. Magnitude and processes of bank erosion at a small stream in Denmark. Hydrol. Process. 25 (10), 1597–1613.
Walker, T.W., Syers, J.K., 1976. The fate of phosphorus during pedogenesis. Geoderma 15 (1), 1–19.
Wei, T., Simko, V., 2021. R package 'corrplot': Visualization of a Correlation Matrix. (Version 0.92), https://github.com/taiyun/corrplot.
Wickham, J., Stehman, S.V., Sorenson, D.G., Gass, L., Dewitz, J.A., 2021. Thematic accuracy assessment of the NLCD 2016 land cover for the conterminous United States. Remote Sens. Environ. 257, 112357.
Yang, X., Post, W.M., 2011. Phosphorus transformations as a function of pedogenesis: A synthesis of soil phosphorus data using Hedley fractionation method. Biogeosciences 8 (10), 2907–2916.
Young, E.O., Ross, D.S., 2016. Total and Labile Phosphorus Concentrations as Influenced by Riparian Buffer Soil Properties. J. Environ. Qual. 45 (1), 294–304.
Young, E.O., Ross, D.S., Alves, C., Villars, T., 2012. Soil and landscape influences on native riparian phosphorus availability in three Lake Champlain Basin stream corridors. J. Soil Water Conserv. 67 (1), 1–7.
Zaimes, G.N., Tufekcioglu, M., Schultz, R.C., 2019. Riparian Land-Use Impacts on Stream Bank and Gully Erosion in Agricultural Watersheds: What We Have Learned. Water 11 (7).
Zhang, Z., Zhao, Z., Liu, C., Chadwick, O.A., Liang, C., Hu, Y., Vaughan, K.L., Zhu, M., 2021. Vertical patterns of phosphorus concentration and speciation in three forest soil profiles of contrasting climate. Geochim. Cosmochim. Acta 310, 1–18.